


Oral delivery of brain-targeted miltefosine-loaded alginate nanoparticles functionalized with polysorbate 80 for the treatment of cryptococcal meningitis

Cristina C. Spadari¹, Dylan M. Lanser², Marcelo V. Araújo¹, Daniel F. F. De Jesus¹, Luciana B. Lopes¹, Angie Gelli² and Kelly Ishida ^{1*}

¹Institute of Biomedical Sciences, University of São Paulo, São Paulo, SP, Brazil; ²Department of Pharmacology, School of Medicine, University of California, Davis, CA, USA

*Corresponding author. E-mail: ishidakelly@usp.br

Received 29 July 2022; accepted 15 February 2023

Objectives: To develop alginate nanoparticles functionalized with polysorbate 80 (P80) as miltefosine carriers for brain targeting in the oral treatment of cryptococcal meningitis.

Methods: Miltefosine-loaded alginate nanoparticles functionalized or not with P80 were produced by an emulsification/external gelation method and the physicochemical characteristics were determined. The haemolytic activity and cytotoxic and antifungal effects of nanoparticles were assessed in an *in vitro* model of the blood–brain barrier (BBB). A murine model of disseminated cryptococcosis was used for testing the efficacy of oral treatment with the nanoparticles. In addition, serum biomarkers were measured for toxicity evaluation and the nanoparticle biodistribution was analysed.

Results: P80-functionalized nanoparticles had a mean size of ~300 nm, a polydispersity index of ~0.4 and zeta potential around –50 mV, and they promoted a sustained drug release. Both nanoparticles were effective in decreasing the infection process across the BBB model and reduced drug cytotoxicity and haemolysis. In *in vivo* cryptococcosis, the oral treatment with two doses of P80 nanoparticles reduced the fungal burden in the brain and lungs, while the non-functionalized nanoparticles reduced fungal amount only in the lungs, and the free miltefosine was not effective. In addition, the P80-functionalization improved the nanoparticle distribution in several organs, especially in the brain. Finally, treatment with nanoparticles did not cause any toxicity in animals.

Conclusions: These results support the potential use of P80-functionalized alginate nanoparticles as miltefosine carriers for non-toxic and effective alternative oral treatment, enabling BBB translocation and reduction of fungal infection in the brain.

Introduction

Cryptococcal meningitis (CM) is an opportunistic fungal infection mainly caused by *Cryptococcus neoformans* that occurs commonly in immunocompromised patients, such as those with advanced HIV infection.^{1,2} Inadequate or no treatment is associated with 81% mortality; however, the mortality rate of patients who have received appropriate antifungal treatment reduces to 20%–30%.¹ The infection begins in the lung through inhalation of yeasts or spores present in the environment. Following the establishment of pulmonary infection, cryptococci disseminate primarily to the CNS upon crossing the blood–brain barrier (BBB).^{3–5}

The recommended therapy for CM is the combination of amphotericin B with flucytosine in the induction phase followed by

fluconazole in the maintenance phase.^{6,7} Besides antifungal therapy being limited to a few drugs, there are problems of significant toxicity and increased resistance.⁸ Furthermore, treatment of CNS infections is often difficult because the BBB limits the diffusion of molecules to the CNS and efflux pumps can reduce drug concentrations in the tissue, resulting in therapeutic failure.⁹ Thus, the need for new treatment options for CM is evident.

Previous *in vitro* and *in vivo* studies showed that miltefosine, an oral FDA-approved treatment of leishmaniasis (2014),¹⁰ also has broad-spectrum activity and fungicidal effects against dimorphic, filamentous and yeast fungi.^{11–21} In female mice with disseminated cryptococcosis, oral miltefosine increased animal survival and reduced the fungal burden;²¹ however, a limited effect was observed in male mice models of CM and disseminated

cryptococcosis.²² Indeed, data on miltefosine antifungal activity in *in vivo* models are scarce and still inconclusive.

Recently, miltefosine was granted 'Orphan Drug' designation by the FDA for the treatments of invasive candidiasis (2021) and primary amoebic meningoencephalitis (2016).²³ However, this drug has some disadvantages, such as limited penetration across the BBB in humans (only 2%–4% of plasma concentration) and high affinity for serum proteins, thus limiting tissue distribution.^{24,25} In addition, miltefosine causes gastrointestinal adverse effects when orally administered and presents renal and hepatic toxicities, a teratogenic effect and high haemolytic activity.²⁴

The use of drug delivery systems has increased in the last few decades as alternative treatments for many diseases, mainly to overcome drug toxicity and pharmacokinetic limitations. Nanocarriers have been increasingly investigated to deliver drugs and macromolecules to the brain as a non-invasive approach to promote transport through the BBB.²⁶ In this regard, nanocarriers can undergo surface modifications to improve drug delivery, and the use of surfactants, such as polysorbate 80 (P80), can increase the ability of nanocarriers to cross the BBB.²⁷ Recently, our research group demonstrated standardized alginate-based nanoparticles as miltefosine carriers as an alternative treatment of cryptococcosis, candidiasis and aspergillosis in a larval model of infection and a murine model of vaginal candidiasis.^{12,28,29} Furthermore, the alginate nanoparticles released miltefosine in a sustained manner, decreased drug toxicity in the larval model, and no haemolytic effect was observed compared with free miltefosine.²⁹ Building upon this work, we functionalized miltefosine-loaded alginate nanoparticles with P80 for brain targeting, and assessed their toxicity, biodistribution and antifungal activity in a human *in vitro* BBB model and in a murine model of systemic cryptococcosis.

Materials and methods

Alginate nanoparticle production

Alginate nanoparticles were produced by emulsification using the external gelation method. The unloaded alginate nanoparticles (AN) and miltefosine-loaded alginate nanoparticles (MFS-AN) were produced according to the protocol previously described.²⁹ The P80-functionalized alginate nanoparticles (P80-AN and P80-MFS-AN) were standardized using the same protocol, except that P80 was included. Briefly, an emulsion with 1.35 g of 1% alginate (MP Biomedicals, USA) and 2.04 g of sunflower oil containing 3% SPAN 80 (Sigma-Aldrich, USA) was prepared, homogenized for 1 min and probe sonicated for 10 min (50 s on—10 s off). Under stirring, 0.2 M calcium chloride with 0.5% P80 (Synth, Brazil) was added and sonicated for 5 min (50 s on—10 s off). After 30 min of stirring, the emulsion was centrifuged for 10 min at 3000 g and the supernatant was removed. Then, 10% trehalose was added to the samples for freeze-drying for 24 h. To obtain P80-MFS-AN, 3 mg of miltefosine (Cayman Chemical, USA) was added to the alginate dispersion.

P80-MFS-AN and MFS-AN nanoparticles were stored at -22°C for 1 to 90 days to evaluate the stability by determination of average diameter (Dz), polydispersity index (Pdi) and zeta potential. Nanoparticles were diluted in distilled water (1:1000, v/v) to determine Dz and Pdi by dynamic light scattering (DLS), while the zeta potential was measured by electrophoresis using a Nano ZS (Malvern Instruments, UK).

Encapsulation efficiency and *in vitro* miltefosine release assay

The encapsulation efficiency of miltefosine in the P80-functionalized alginate nanoparticles was obtained by quantification of miltefosine

remaining in the supernatant. To assess drug release, P80-MFS-AN nanoparticles were dispersed in 1 mL of sterile distilled water and incubated at 37°C under constant agitation (200 rpm). At 6, 12 and 24 h, the samples were centrifuged for 5 min at 3000 g and the supernatants were collected for miltefosine quantification. Miltefosine was quantified colorimetrically at 460 nm (Epoch 2, BioTek, USA) based on a miltefosine calibration curve (15.62 to 2000 mg/L).³⁰ The encapsulation percentage was calculated using the formula: $100 - (\text{miltefosine in supernatant} \times 100 / \text{amount of initial miltefosine})$.²⁹

Antifungal susceptibility test

The MIC values of miltefosine, in its free form and loaded in nanoparticles (P80-MFS-AN) were determined by the broth microdilution technique³¹ against *C. neoformans* H99. MIC was defined as the lowest concentration that inhibited 90% of fungal growth by visual inspection.

Haemolytic activity

A 4% suspension of RBCs (v/v, in 5% glucose-PBS) was subjected to treatment with various concentrations of miltefosine and P80-MFS-AN nanoparticles for 2 h in a bath at 37°C . The negative (no treatment) and positive (0.1% Triton X-100) controls were included in the test for haemolytic activity (HA) determination,²⁹ and 50% HA (HA_{50}) was obtained by linear prediction.

In vitro BBB model

Antifungal effect

Endothelial cells (hCMEC/D3 passages 25–30) were seeded at 50% confluent density on collagen-coated permeable transwell inserts (Corning, USA; 8 μm pore diameter) in endothelial basal media (Lonza, USA) supplemented with human fibroblast growth factor (Gibco, USA; 1 ng/mL), 2.5% FBS and antibiotics. After reaching confluence at 4 days, growth factors were reduced first to 50% for 24 h, then to 25% 24 h prior to treatment. Transwells were treated with miltefosine (2 mg/L) or miltefosine-loaded alginate nanoparticles (MFS-AN or P80-MFS-AN; 100 mg/L miltefosine) added to the top of inserts, along with 3.3×10^4 *C. neoformans* H99. After 12 h incubation at 37°C and 5% CO_2 , cfu count beneath the transwell inserts were determined by plating on Sabouraud dextrose agar.

Cytotoxicity

Endothelial cells were grown in 96-well, opaque-wall, clear-bottom plates under the conditions described above. Miltefosine (1.56 to 25 mg/L), MFS-AN or P80-MFS-AN (50 to 800 mg/L miltefosine) were diluted in serum-free media and introduced to triplicate wells. After 24 h incubation at 37°C , 5% CO_2 , cytotoxicity was evaluated with an MTT assay kit (Abcam, USA), and calculated as $\% \text{cytotoxicity} = 100 \times [(\text{absorbance of control}) - (\text{absorbance of treatments})] / (\text{control absorbance})$.

In vivo experiments

Male BALB/c mice aged 6–8 weeks with an average weight of 25 g were kept in pathogen-free conditions with water and food *ad libitum* in the Animal Experimentation Vivarium of the Departments of Parasitology and Microbiology (ICB/USP). All experimental protocols were previously approved by the Ethics Committee for Animal Use of the Institute of Biomedical Sciences (CEUA-ICB/USP, Reg 68/2014).

Antifungal activity and toxicity of alginate nanoparticles in a murine model of systemic cryptococcosis

C. neoformans H99 yeast was cultivated twice in Sabouraud dextrose broth for 72 h at 35°C . A yeast suspension was adjusted to 1×10^7 cfu/mL of PBS

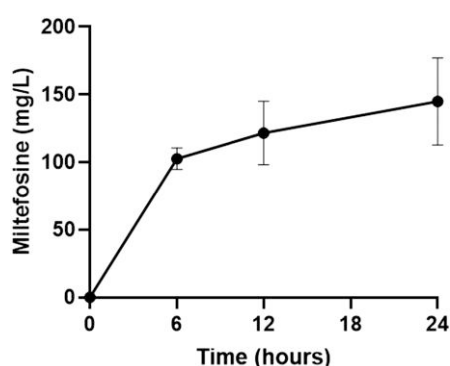


Figure 1. *In vitro* miltefosine release from polysorbate 80-functionalized alginate nanoparticles. The miltefosine quantification, in the supernatant, was performed by the colorimetric method with ammonium ferri-thiocyanate.³⁰ The experiment was performed three times in triplicate.

for inoculation of 100 μ L into the tail vein of the mice. After 1 h of infection, the animals (five per group) were orally treated by gavage with 100 μ L of three treatments: (i) 10 mg/kg miltefosine, in water, once a day for 5 days (miltefosine group); (ii) 20 mg/kg miltefosine-loaded alginate nanoparticles, in PBS, after 1 and 72 h of infection (MFS-AN group); and (iii) 20 mg/kg miltefosine-loaded P80-functionalized alginate nanoparticles, in PBS, after 1 and 72 h of infection (P80-MFS-AN group).

On the sixth day after infection, the animals were euthanized with a lethal dose of anaesthetics (xylazine 30 mg/kg and ketamine 900 mg/kg). The organs (lung and brain) were excised, weighed, macerated in PBS, and plated on Sabouraud dextrose agar with 50 mg/L chloramphenicol and incubated at 35°C for 72 h for cfu count. During organ removal, a fraction of each tissue was separated, fixed in 10% formalin and processed for histopathological analysis using Gomori-Grocott staining.²⁸

Additionally, after euthanasia the blood was collected and the serum obtained was used for measurement of glucose, triglycerides, cholesterol, creatinine, urea, alkaline phosphatase (ALP), AST and ALT. In addition, a non-infected and non-treated group (NINT), i.e. mice that did not suffer any procedure ($n=5$), was included in this assay. The analyses were carried out by the wet biochemistry method (Equipment Urit 8210, URIT Medical, China).

Biodistribution of alginate nanoparticles

Production of fluorescent nanoparticles

Alginate nanoparticles were produced according to the protocols described above, except that 5 mg of rhodamine B (Rod) (Sigma-Aldrich, USA) was added to the alginate dispersion to obtain the fluorescent nanoparticles, modified or not with polysorbate 80 (P80-AN-Rod and AN-Rod, respectively).

Biodistribution assay

One hundred microlitres of P80-AN-Rod or AN-Rod, dispersed in PBS, were orally administered by gavage. Animals that received PBS-Rod solution (Rod group) or only PBS (PBS group) were included as control groups. After 12 and 24 h, the animals were euthanized with a lethal dose of anaesthetics. The organs were removed for evaluation of fluorescence in a bioimaging system (IVIS Spectrum System, Perkin-Elmer Life Sciences, USA) using an exposure time of 1 s and excitation/emission wavelengths of 535/580 nm. After that, the organs were macerated with 1 mL of PBS and 100 μ L added to the wells of the 96-well polystyrene flat-bottom plate for fluorescence quantification in the plate reader (Synergy/

H1, BioTek, USA) at excitation/emission wavelengths of 535/580 nm, resulting in fluorescence measured in relative fluorescence units (RFU).

Statistical analyses

The statistical analyses were performed using the GraphPad Prism version 8.0 (GraphPad Software, USA) and a P value less than 0.05 was considered significant.

Results

P80-functionalization does not alter the average size and polydispersity of alginate nanoparticles and increases stability

Both nanoparticles P80-MFS-AN and MFS-AN had similar D_z (~300 nm) and P_{di} (~0.4), and the P80 functionalization increased the absolute value of zeta potential. In addition, the freeze-drying step did not interfere with these parameters (Table S1, available as Supplementary data at JAC Online).

The size and P_{di} values of P80-MFS-AN nanoparticles did not change during 60 days of storage, but after 75 and 90 days, the size increased 1.2-fold ($P<0.05$) although no changes to the dispersion were noticed (Figure S1). Compared with P80-functionalized nanoparticles, the MFS-AN displayed more pronounced increases in size and P_{di} at shorter periods of time. More specifically, 1.8- and 1.92-fold increases in size and P_{di} , respectively, at 60 days, and 1.92- and 2.28-fold in size and P_{di} , at 90 days, respectively, were observed ($P<0.001$) (Figure S1).

P80-alginate nanoparticles encapsulate miltefosine and promote its sustained *in vitro* release

The encapsulation efficiency of miltefosine in P80-functionalized alginate nanoparticles was $73.20\% \pm 9.89\%$. P80-MFS-AN nanoparticles promoted a sustained release of miltefosine with an increase in concentration over the first 6 h, obtaining a peak release of approximately 102.65 mg/L in 6 h. After this period, the drug release was slow and prolonged with a peak value (~144.87 mg/L) at 24 h (Figure 1).

Alginate nanoparticles reduce miltefosine haemolytic activity and cytotoxicity on endothelial cells

The haemolytic effect of miltefosine was concentration dependent (Figure 2a) and its HA_{50} value was ~43.6 mg/L. Unloaded and miltefosine-loaded nanoparticles (P80-MFS-AN) did not cause any haemolytic effect, even at the highest tested miltefosine concentration (128 mg/L), which is consistent with previously obtained results for MFS-AN.²⁹

Increases in miltefosine concentration also increased its cytotoxic effects in an *in vitro* BBB model with hCMEC/D3 endothelial cells (Figure 2b and c). Compared with miltefosine, which presented a CC_{50} of 8.67 mg/L, drug encapsulation in nanoparticles drastically reduced its cytotoxic effect and increased the CC_{50} by 38.4- and 45.12-fold for MFS-AN and P80-MFS-AN, respectively. In addition, concentrations less than or equal to 3.12 mg/L miltefosine and 100 mg/L miltefosine-loaded nanoparticles (P80-MFS-AN and MFS-AN) resulted in low and insignificant cell damage ($P>0.05$, Figure 2b and c).

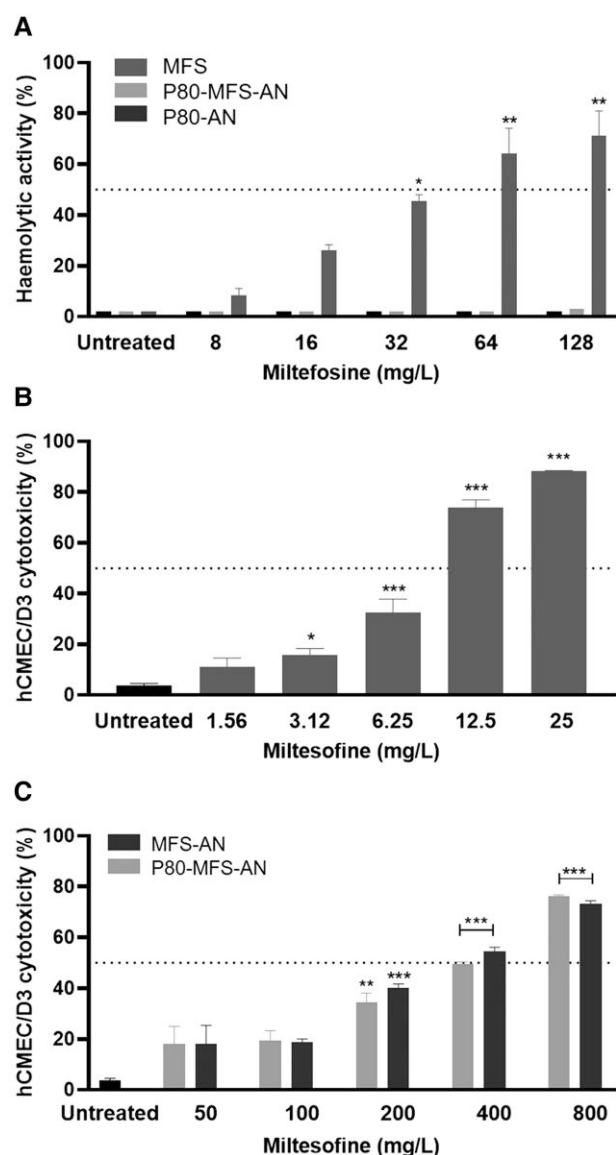


Figure 2. Cytotoxicity of miltefosine (MFS) in its free form or loaded on alginate nanoparticles. (a) Haemolytic activity of MFS and MFS-loaded alginate nanoparticles, functionalized or not with polysorbate 80 (P80-MFS-AN and MFS-AN, respectively). (b) Cytotoxicity of MFS and (c) P80-MFS-AN and MFS-AN on hCMEC/D3 endothelial cells. * $P < 0.05$, ** $P < 0.01$ and *** $P < 0.001$ versus untreated group (one-way ANOVA with Dunnett's post-test). The assays were performed three times in triplicate.

In vitro antifungal activity using a BBB model

The MIC values of miltefosine, in its free form and loaded in nanoparticles (P80-MFS-AN) were 2 and 100 mg/L for *C. neoformans*. Unloaded P80-AN nanoparticles were evaluated as a control and no inhibitory effect was observed.

After cytotoxicity assays and MIC determination, the antifungal activity of 2 mg/L miltefosine and 100 mg/L miltefosine-loaded nanoparticles (MFS-AN and P80-MFS-AN) was evaluated in the *in vitro* BBB model infected with *C. neoformans*. After 12 h, all treatments were significantly effective in reducing fungal viability compared with the untreated group ($P < 0.001$, Figure 3).

P80-functionalized alginate nanoparticles decrease fungal burden in the brain and lung in a murine model of systemic cryptococcosis

The oral treatment with P80-MFS-AN nanoparticles significantly decreased the fungal burden in the brain (~ 1.8 log, $P < 0.05$) and lung (~ 1 log, $P < 0.05$) when compared with the untreated group (Figure 4a and b). MFS-AN nanoparticles significantly decreased the fungal burden in the lungs (~ 1 log, $P < 0.05$), but failed to significantly reduce it in the brain when compared with the untreated group (Figure 4a and b). On the other hand, the oral miltefosine treatment was the least effective, reducing only ~ 0.5 log of fungal burden in the lung and brain of animals (Figure 4a and b). These cfu results corroborated the semi-quantitative data obtained from histopathological analysis, which demonstrated that P80-MFS-AN treatment led to a lower amount of yeast in the brain and lung of the animals, highlighting it as the best antifungal therapy in the murine model of systemic cryptococcosis (Figure 4c–j). In addition, no significant difference was observed in hepatic (AST, ALT and ALP) and renal (creatinine and urea) toxicity biomarkers as well as glucose, triglycerides and cholesterol levels when compared with the NINT group (Table 1).

P80-functionalization increases the biodistribution of alginate nanoparticles and enhances their presence in the brain, suggesting improved translocation across the BBB

To evaluate the biodistribution of alginate nanoparticles, P80 functionalized or not, we encapsulated a fluorescent marker rhodamine. As expected, little or no fluorescence was detected in the organs of animals that received only PBS. While rhodamine, *per se*, was absorbed and distributed to some organs, the fluorescence intensity was much lower than for animals that received alginate nanoparticles (Figure 5).

The qualitative analysis of the organs' fluorescence was performed in a bioimaging system at 12 h after oral administration of nanoparticles (Figure 5a). P80 functionalization of alginate nanoparticles (P80-AN-Rod) had a larger biodistribution, observed in almost all analysed organs (heart, lungs, kidneys, liver, pancreas, stomach, testicle, intestine and brain) (Figure 5a). On the other hand, alginate nanoparticles (AN-Rod) were detected in the liver, pancreas, stomach, testicle and intestine (Figure 5a). At 24 h, the organs' fluorescence reduced to control PBS and rhodamine levels.

Importantly, the fluorescence results were confirmed in a plate reader as the method is more sensitive for quantification of fluorescence (Figure 5b). Indeed, P80-functionalized alginate nanoparticles were detected in all organs, with higher amounts in the brain, while non-functionalized alginate nanoparticles were found in the kidneys, spleen and liver; in the lungs and pancreas, they were found in greater amounts than P80 functionalized nanoparticles (Figure 5b).

Discussion

The use of nanoparticle-mediated drug delivery systems functionalized with ligands targeting the CNS for the treatment of brain diseases has been increasing.²⁶ For fungal brain diseases, few antifungals have suitable CNS penetration with adequate

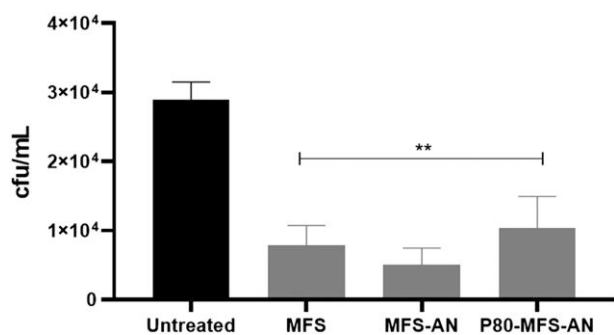


Figure 3. Antifungal activity of miltefosine (MFS), in its free form or loaded on alginate nanoparticles, during *C. neoformans* infection across the BBB transwell model (hCMEC/D3 cells). Fungal burden (cfu/mL) was recovered from the basal compartment of the transwell after 12 h of infection and treatment with free MFS (2 mg/L) and MFS-loaded alginate nanoparticles, functionalized or not with polysorbate 80 (P80-MFS-AN and MFS-AN, respectively) (100 mg/L MFS). ** $P < 0.001$ versus untreated group (one-way ANOVA with Dunnett's post-test). The experiment was performed three times in triplicate.

concentrations.⁹ Here, we chose P80, due to its low cost, commercial availability and ease of handling.³² We produced alginate nanoparticles that were P80 functionalized as miltefosine carriers (P80-MFS-AN) that improved antifungal activity in CM treatment when compared with unfunctionalized alginate nanoparticles (MFS-AN).

The physicochemical characteristics of the nanoparticles are important parameters that have an impact on the systemic activities of the nanocarriers,³³ and the P80-MFS-AN nanoparticles had a Dz and Pdi similar to those previously observed for MFS-AN.²⁹ The P80-MFS-AN showed the absolute value of zeta potential increased to approximately -50 mV. This is an important feature since zeta potential higher than 30 mV (in module) has been associated with greater electrical stability and lower particle aggregation.^{34,35} The higher zeta potential of P80-MFS-AN compared with MFS-AN may have contributed to its enhanced stability.

The toxicity of miltefosine has been described in previous reports;²⁴ the haemolytic effect and cytotoxicity on hCMEC/D3 endothelial cells at low concentrations corroborate previous observations. In contrast, the use of alginate nanoparticles as miltefosine carriers reduced its cytotoxicity considerably, abolishing the haemolytic effect and increasing the CC_{50} values in hCMEC/D3 cells 38–45 times. Drug delivery systems usually reduce the toxic effect of drugs, as observed in this work and by other authors who incorporated miltefosine in delivery systems.^{36–38}

The *in vitro* antifungal activity of P80-MFS-AN was similar to that observed for MFS-AN with high values compared with miltefosine.²⁹ This is expected in *in vitro* assays and can be explained by the slow and sustained release of the drug, also observed in other studies that tested antifungal nanocarriers.^{39,40} Additionally, in an *in vitro* BBB model, the miltefosine and miltefosine-loaded nanoparticles were effective in decreasing *C. neoformans*' viability during infection. The hCMEC/D3 immortalized brain endothelial cell line is an alternative to *in vivo* studies of the BBB, which has already been used for research of *C. neoformans* invasion in the CNS.⁴¹ In this model, it was possible to observe that miltefosine and miltefosine-loaded alginate nanoparticles decreased the

passage of fungus through the BBB, a very important step in the disease and that, for reasons not yet well known, this fungus has a special tropism for the brain and can invade the BBB by different and concomitant mechanisms.⁵

The use of nanoparticles for drug delivery to the brain is a promising alternative due to the possibility of surface multifunctionalization that can promote the targeting or/and crossing enhancement to the BBB.⁴² Among functionalization options is the use of surfactants, with polysorbates being the most efficient for targeting to the brain when compared with poloxamers, poloxamine 908, Cremophor[®] EZ, Cremophor[®] RH 40, polyoxyethylene-(23)-lauryl ether (Brij[®] 35).⁴³ Consistent with previous reports, MFS-AN nanoparticles, which were prepared with poloxamer 407,²⁹ did not reach the brain in adequate amounts to control the cerebral infection. In contrast, P80-MFS-AN nanoparticles, which were functionalized with P80, showed greater biodistribution and crossed the BBB, reaching the brain in higher amounts and resulting in a significant reduction in fungal burden to undetectable levels.

Our findings corroborated other studies that used P80 for functionalization of amphotericin B-loaded polymeric nanoparticles, enabling the nanoparticles to cross the BBB and increase drug concentrations in brains of mice,⁴⁴ whereas free amphotericin B was not detected. As a result, treatment of cryptococcosis with these nanoparticles decreased the fungal burden and increased the survival rate of animals to 80%.⁴⁵ In addition, a nanoemulsion with 3% surfactant blend containing Tween[®] 80 and Soluplus[®] and incorporating flubendazole (an anthelmintic reported to have antifungal activity) was effective when orally administered in murine systemic cryptococcosis, decreasing the fungal burden in the brain by 30%.⁴⁶

Several mechanisms have been proposed to explain the efficiency of nanoparticles to pass through the BBB.^{47,48} For surfactant-functionalized nanoparticles, e.g. polysorbate 80, the previously proposed mechanism is based on the solubilization of lipids in the endothelial cell membrane that would lead to fluidization and destabilization of the membrane and greater permeability of the nanoparticles through the BBB.^{47,48} Additionally, this general effect of surfactants might contribute to the wider biodistribution of P80-functionalized alginate nanoparticles in mice compared with the non-functionalized nanoparticles. This finding might open up new possibilities for therapeutic applications of P80-MFS-AN nanoparticles, such as for the treatment of leishmaniasis and other systemic fungal infections. On the other hand, because wider distribution might lead to more side effects, we also addressed toxicological concerns by assessing markers of hepatic and renal damage. Biochemical analysis of serum after treatment with miltefosine and miltefosine-loaded alginate nanoparticles indicated that hepatic and renal markers, as well as markers of carbohydrate and lipid metabolism were not altered after treatments. These data support the idea that nanoparticles, in the therapeutic scheme used here, are safe to treat CM.

It is important to highlight that oral administration of P80-MFS-AN nanoparticles (two doses, 1 and 72 h after infection) were the best therapy to reduce fungal burden in the brain and lungs while the oral free miltefosine (five doses, 24/24 h) was ineffective to control the infection in systemic cryptococcosis as well as observed previously in CM and disseminated cryptococcosis models treated orally with miltefosine.²² Our data differ

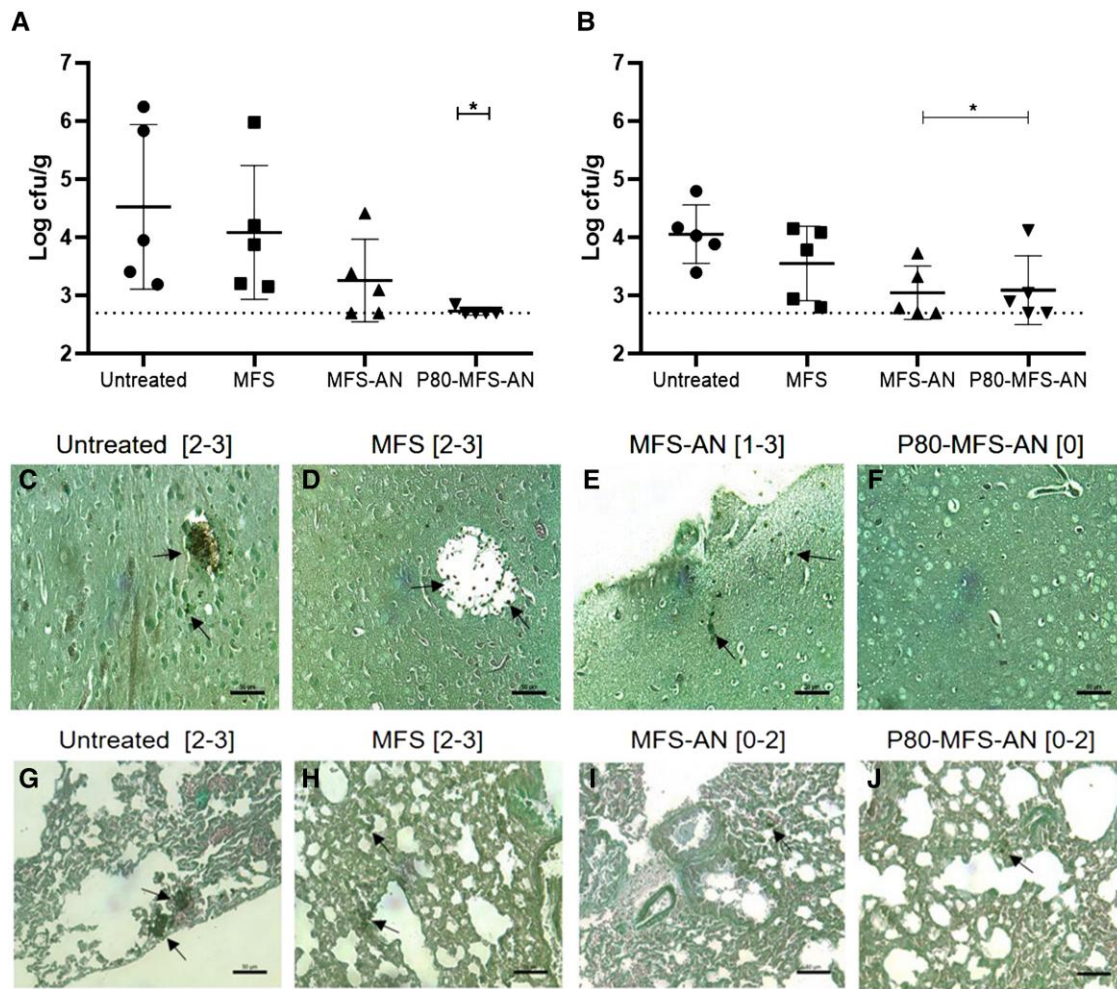


Figure 4. Antifungal effect of miltefosine (MFS), in its free form or loaded on alginate nanoparticles, in the murine model of systemic cryptococcosis. Fungal burden in the brain (a) and lungs (b) of male mice infected with *C. neoformans* H99 untreated and treated with MFS or MFS-loaded alginate nanoparticles (MFS-AN and P80-MFS-AN). * $P < 0.05$ versus untreated group (one-way ANOVA with Dunnett's post-test). Gomori-Grocott-stained histopathological sections of brain (c-f) and lungs (g-j) of the animals untreated and treated with MFS, MFS-AN or P80-MFS-AN. Results of semi-quantitative fungal load analysis from brain and lung tissue sections are indicated in brackets according to the scale: 0, no fungal load; 1, up to 5 fungal elements per section; 2, ≥ 6 fungal elements per section; 3, from 6 to 50 fungal elements per field; and 4, more than 50 fungal elements per field.²⁸ Bars = 50 μm . Arrows indicate the fungal cells. This figure appears in colour in the online version of JAC and in black and white in the print version of JAC.

Table 1. Serum biomarkers of mice infected by *C. neoformans* and treated with miltefosine (MFS) or MFS-loaded alginate nanoparticles functionalized or not with polysorbate 80 (P80-MFS-AN and MFS-AN, respectively)

Biomarkers	NINT	Untreated	MFS	MFS-AN	P80-MFS-AN
Urea (mg/dL)	56.76 \pm 7.77	49.84 \pm 2.70	64.32 \pm 18.56	49.76 \pm 9.35	52.70 \pm 9.66
Creatinine (mg/dL)	0.69 \pm 0.08	0.68 \pm 0.15	0.80 \pm 0.06	0.78 \pm 0.12	0.67 \pm 0.09
AST (U/L)	268 \pm 102.9	263.2 \pm 249.7	265.8 \pm 222.4	329.2 \pm 283.8	197.2 \pm 128.5
ALT (U/L)	49.50 \pm 6.6	44.40 \pm 18.62	52 \pm 25.14	62.20 \pm 23.44	43.20 \pm 17.92
ALP (U/L)	518.4 \pm 55.61	390.8 \pm 83.79	361.6 \pm 48.63	424.8 \pm 114	375.2 \pm 73.02
Glucose (mg/dL)	367.2 \pm 94.28	258.8 \pm 79.26	209.8 \pm 52.96	271 \pm 37.87	293.8 \pm 32.15
Triglycerides (mg/dL)	211.4 \pm 52.86	176 \pm 19.52	208.3 \pm 60.42	186.7 \pm 44.83	194.7 \pm 87.50
Cholesterol (mg/dL)	109.7 \pm 8.57	106.6 \pm 11.56	138.7 \pm 47.13	121.6 \pm 13.59	119.3 \pm 6.43

All values are given as mean \pm SD.

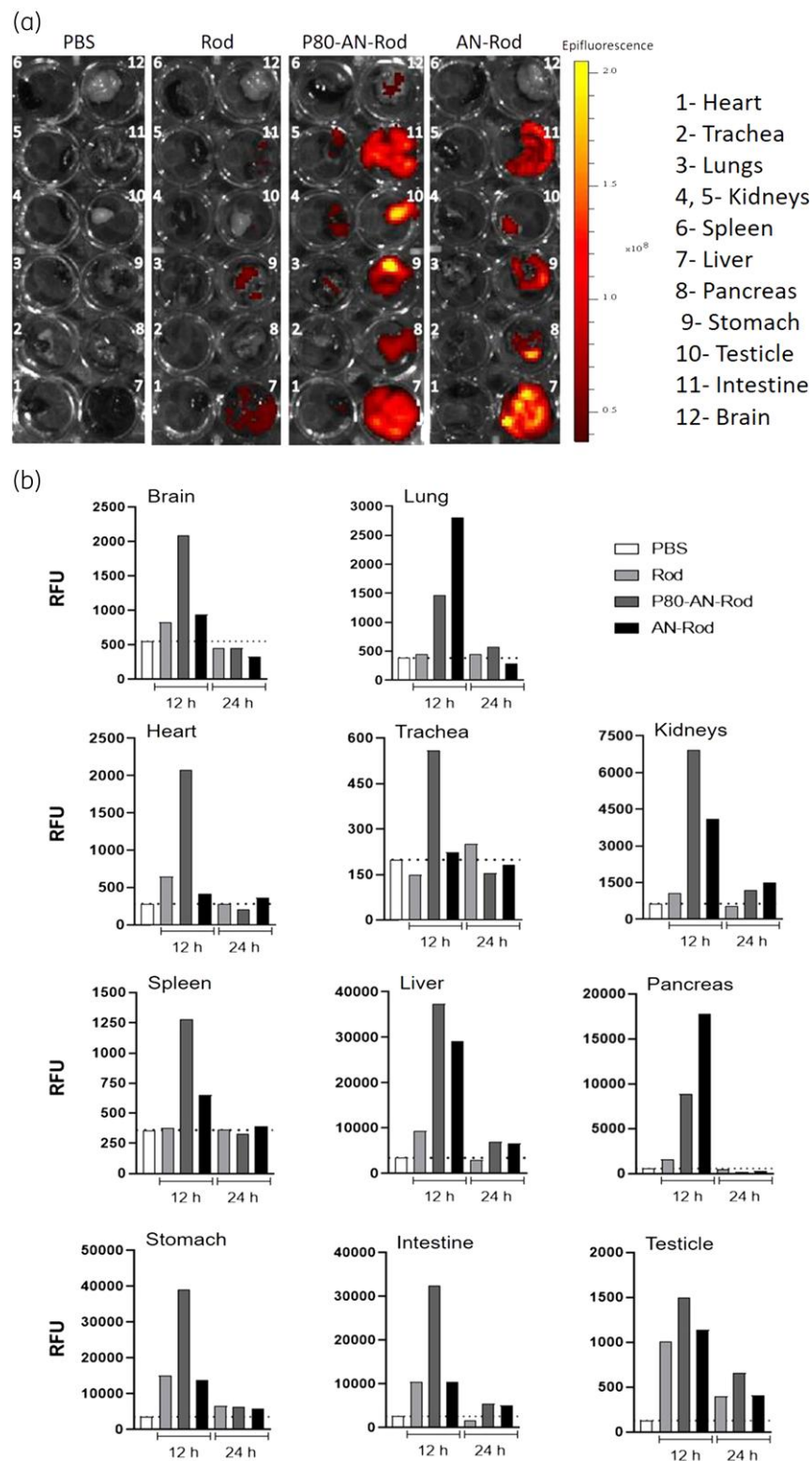


Figure 5. Biodistribution of alginate nanoparticles, functionalized or not with polysorbate 80. (a) Fluorescent images obtained in a bioimaging system of the organs of mice treated with rhodamine-loaded alginate nanoparticles without (AN-Rod) and with polysorbate 80 (P80-AN-Rod) at 12 h. (b) RFU of organs from mice treated with AN-Rod or P80-AN-Rod obtained at excitation/emission wavelengths of 535/580 nm at 12 and 24 h. Rhodamine B (Rod) and PBS were used as controls. These data are representative of an experiment carried out twice. This figure appears in colour in the online version of *JAC* and in black and white in the print version of *JAC*.

from results reported by Widmer and co-workers,²¹ although the murine model used here was similar, except the mice gender (they used female mice). It was reported that steroid hormones affect *C. neoformans* virulence,⁴⁹ and oestradiol, a female hormone, is associated with a protective factor against *Cryptococcus* infection.⁵⁰

Notably, the alginate nanoparticles, especially P80-functionalized ones, improved the *in vivo* antifungal effect of miltefosine when compared with miltefosine in solution. Moreover, the increase in dose interval used here resulted from the nanoparticle ability to modify and slow down the release of miltefosine. This is consistent with the drug release profile observed from non-functionalized nanoparticles (MFS-AN)²⁹ and other alginate-based carriers.^{51,52} This feature visibly was relevant at decreasing *Candida albicans* infection, and a single dose of MFS-AN was sufficient to treat vaginal candidiasis in a murine model.²⁸

In conclusion, P80-MFS-AN represents a safe oral delivery system to improve the brain delivery of miltefosine in CM treatment. In addition, the nanoparticles promoted sustained release of miltefosine, were more widely biodistributed, including in the brain, and decreased brain fungal burden without producing detectable damage to other organs. This study demonstrates that it is possible to obtain new management strategies for treatment of CM. Finally, our results open many other questions regarding the efficacy of combined treatment of P80-MFS-AN with standard antifungals (amphotericin B, flucytosine and/or fluconazole) and pharmacokinetic/pharmacodynamic data. Further studies must be conducted to bring promising results to improve CNS treatments and support the clinical trials.

Acknowledgements

We would like to thank Marcela Gonçalves for her assistance in preparation of mice samples for histopathological analysis. IVIS analysis was conducted at the CEFAP core facility (Institute of Biomedical Sciences, University of São Paulo).

Funding

This study was supported by Fundação de Amparo a Pesquisa do Estado de São Paulo (FAPESP, Brazil, 2021/01279-5 and 2018/13877-1), Conselho Nacional de Desenvolvimento Científico e Tecnológico (CNPq, Brazil), Coordenação de Aperfeiçoamento de Pessoal de Nível Superior (CAPES, Brazil) and National Institute of Health (NINDS, USA, NS110800). C.C.S. was FAPESP fellow (2018/12149-2) and D.F.F.J. was CAPES fellow (finance code 001). K.I. and L.B.L. are research fellows of the CNPQ (303373/2019-9 and 306866/2020-0, respectively).

Transparency declarations

None to declare.

Author contributions

C.C.S. performed the experiments, analysed the results, and wrote the manuscript. M.V.A. and D.F.F.J. contributed with murine model assays. D.M.L. did the blood-brain barrier experiments. K.I., A.G. and L.B.L. designed the experiments, performed data critical review, and wrote and edited the manuscript. All authors have read and approved the manuscript before publication.

Data availability

All data will be made available from the corresponding author upon request.

Supplementary data

Figure S1 and Table S1 are available as [Supplementary data](#) at JAC Online.

References

- Rajasingham R, Smith RM, Park BJ *et al.* Global burden of disease of HIV-associated cryptococcal meningitis: an updated analysis. *Lancet Infect Dis* 2017; **17**: 873–81. [https://doi.org/10.1016/S1473-3099\(17\)30243-8](https://doi.org/10.1016/S1473-3099(17)30243-8)
- Stott KE, Loyse A, Jarvis JN *et al.* Cryptococcal meningoencephalitis: time for action. *Lancet Infect Dis* 2021; **21**: e259–71. [https://doi.org/10.1016/S1473-3099\(20\)30771-4](https://doi.org/10.1016/S1473-3099(20)30771-4)
- Lin X, Heitman J. The biology of the *Cryptococcus neoformans* species complex. *Annu Rev Microbiol* 2006; **60**: 69–105. <https://doi.org/10.1146/annurev.micro.60.080805.142102>
- O'Meara TR, Alspaugh JA. The *Cryptococcus neoformans* capsule: a sword and a shield. *Clin Microbiol Rev* 2012; **25**: 387–408. <https://doi.org/10.1128/CMR.00001-12>
- Zaragoza O. Basic principles of the virulence of *Cryptococcus*. *Virulence* 2019; **10**: 490–501. <https://doi.org/10.1080/21505594.2019.1614383>
- May RC, Stone NRH, Wiesner DL *et al.* *Cryptococcus*: from environmental saprophyte to global pathogen. *Nat Rev Microbiol* 2016; **14**: 106–17. <https://doi.org/10.1038/nrmicro.2015.6>
- Perfect JR, Dismukes WE, Dromer F *et al.* Clinical practice guidelines for the management of cryptococcal disease: 2010 update by the Infectious Diseases Society of America. *Clin Infect Dis* 2010; **50**: 291–322. <https://doi.org/10.1086/649858>
- Campoy S, Adrio JL. Antifungals. *Biochem Pharmacol* 2017; **133**: 86–96. <https://doi.org/10.1016/j.bcp.2016.11.019>
- Wirth F, Ishida K. Antifungal drugs: an updated review of central nervous system pharmacokinetics. *Mycoses* 2020; **63**: 1047–59. <https://doi.org/10.1111/myc.13157>
- Sunyoto T, Potet J, Boelaert M. Why miltefosine—a life-saving drug for leishmaniasis—is unavailable to people who need it the most. *BMJ Glob Heal* 2018; **3**: e000709. <https://doi.org/10.1136/bmjgh-2018-000709>
- Barreto TL, Rossato L, de Freitas ALD *et al.* Miltefosine as an alternative strategy in the treatment of the emerging fungus *Candida auris*. *Int J Antimicrob Agents* 2020; **56**: 106049. <https://doi.org/10.1016/j.ijantimicag.2020.106049>
- Barreto TL, Lopes LB, Melo ASA *et al.* *In vivo* synergism of free miltefosine or in alginate-based nanocarrier combined with voriconazole on aspergillosis. *Future Microbiol* 2021; **16**: 1153–60. <https://doi.org/10.2217/fmb-2021-0056>
- Borba-Santos LP, Gagini T, Ishida K *et al.* Miltefosine is active against *Sporothrix brasiliensis* isolates with *in vitro* low susceptibility to amphotericin B or itraconazole. *J Med Microbiol* 2015; **64**: 415–22. <https://doi.org/10.1099/jmm.0.000041>
- Brilhante RSN, Malaquias ADM, Caetano ÉP *et al.* *In vitro* inhibitory effect of miltefosine against strains of *Histoplasma capsulatum* var. *capsulatum* and *Sporothrix* spp. *Med Mycol* 2014; **52**: 320–5. <https://doi.org/10.1093/mmy/myt027>
- Compain F, Botterel F, Sitterlé E *et al.* *In vitro* activity of miltefosine in combination with voriconazole or amphotericin B against clinical isolates

- of *Scedosporium* spp. *J Med Microbiol* 2015; **64**: 309–11. <https://doi.org/10.1099/jmm.0.000019>
- 16** Imbert S, Palous M, Meyer I et al. *In vitro* combination of voriconazole and miltefosine against clinically relevant molds. *Antimicrob Agents Chemother* 2014; **58**: 6996–8. <https://doi.org/10.1128/AAC.03212-14>
- 17** Loreto ES, Tondolo JSM, Oliveira DC et al. *In vitro* activities of miltefosine and antibacterial agents from the macrolide, oxazolidinone, and pleuromutilin classes against *Pythium insidiosum* and *Pythium aphanidermatum*. *Antimicrob Agents Chemother* 2018; **62**: e01678-17. <https://doi.org/10.1128/AAC.01678-17>
- 18** Rossi DCP, Spadari CC, Nosanchuk JD et al. Miltefosine is fungicidal to *Paracoccidioides* spp. yeast cells but subinhibitory concentrations induce melanisation. *Int J Antimicrob Agents* 2017; **49**: 465–71. <https://doi.org/10.1016/j.ijantimicag.2016.12.020>
- 19** Spadari CC, Vila T, Rozental S et al. Miltefosine has a postantifungal effect and induces apoptosis in *Cryptococcus* yeasts. *Antimicrob Agents Chemother* 2018; **62**: e00312-18. <https://doi.org/10.1128/AAC.00312-18>
- 20** Tong Z, Widmer F, Sorrell TC et al. *In vitro* activities of miltefosine and two novel antifungal biscationic salts against a panel of 77 dermatophytes. *Antimicrob Agents Chemother* 2007; **51**: 2219–22. <https://doi.org/10.1128/AAC.01382-06>
- 21** Widmer F, Wright LC, Obando D et al. Hexadecylphosphocholine (miltefosine) has broad-spectrum fungicidal activity and is efficacious in a mouse model of cryptococcosis. *Antimicrob Agents Chemother* 2006; **50**: 414–21. <https://doi.org/10.1128/AAC.50.2.414-421.2006>
- 22** Wiederhold NP, Najvar LK, Bocanegra R et al. Limited activity of miltefosine in murine models of cryptococcal meningoencephalitis and disseminated cryptococcosis. *Antimicrob Agents Chemother* 2013; **57**: 745–50. <https://doi.org/10.1128/AAC.01624-12>
- 23** Profounda, Inc. Profounda blog. <https://www.profounda.com/blog>.
- 24** Dorlo TPC, Balasegaram M, Beijnen JH et al. Miltefosine: a review of its pharmacology and therapeutic efficacy in the treatment of leishmaniasis. *J Antimicrob Chemother* 2012; **67**: 2576–97. <https://doi.org/10.1093/jac/dks275>
- 25** Roy SL, Atkins JT, Gennuso R et al. Assessment of blood-brain barrier penetration of miltefosine used to treat a fatal case of granulomatous amebic encephalitis possibly caused by an unusual *Balamuthia mandril-laris* strain. *Parasitol Res* 2015; **114**: 4431–9. <https://doi.org/10.1007/s00436-015-4684-8>
- 26** Ahlawat J, Guillama Barroso G, Masoudi Asil S et al. Nanocarriers as potential drug delivery candidates for overcoming the blood-brain barrier: challenges and possibilities. *ACS Omega* 2020; **5**: 12583–95. <https://doi.org/10.1021/acsomega.0c01592>
- 27** Sun W, Xie C, Wang H et al. Specific role of polysorbate 80 coating on the targeting of nanoparticles to the brain. *Biomaterials* 2004; **25**: 3065–71. <https://doi.org/10.1016/j.biomaterials.2003.09.087>
- 28** de Bastiani FWMDS, Spadari CC, de Matos JKR et al. Nanocarriers provide sustained antifungal activity for amphotericin B and miltefosine in the topical treatment of murine vaginal candidiasis. *Front Microbiol* 2020; **10**: 2976. <https://doi.org/10.3389/fmicb.2019.02976>
- 29** Spadari CC, de Bastiani FWMDS, Lopes LB et al. Alginate nanoparticles as non-toxic delivery system for miltefosine in the treatment of candidiasis and cryptococcosis. *Int J Nanomedicine* 2019; **14**: 5187–99. <https://doi.org/10.2147/IJN.S205350>
- 30** Dorlo TPC, Eggelte TA, de Vries PJ et al. Characterization and identification of suspected counterfeit miltefosine capsules. *Analyst* 2012; **137**: 1265. <https://doi.org/10.1039/c2an15641e>
- 31** CLSI. *Reference Method for Broth Dilution Antifungal Susceptibility Testing of Yeasts—Fourth Edition: M27*. 2017.
- 32** Ravichandran V, Lee M, Nguyen Cao TG et al. Polysorbate-based drug formulations for brain-targeted drug delivery and anticancer therapy. *Appl Sci* 2021; **11**: 9336. <https://doi.org/10.3390/app11199336>
- 33** Raval N, Maheshwari R, Kalyane D et al. Importance of physico-chemical characterization of nanoparticles in pharmaceutical product development. In: *Basic Fundamentals of Drug Delivery*. Elsevier, 2019; 369–400.
- 34** Sundar S, Kundu J, Kundu SC. Biopolymeric nanoparticles. *Sci Technol Adv Mater* 2010; **11**: 014104. <https://doi.org/10.1088/1468-6996/11/1/014104>
- 35** Honary S, Zahir F. Effect of zeta potential on the properties of nano-drug delivery systems—a review (Part 1). *Trop J Pharm Res* 2013; **12**: 265–73. <https://doi.org/10.4314/tjpr.v12i2.19>
- 36** da Gama Bitencourt JJ, Pazin WM, Ito AS et al. Miltefosine-loaded lipid nanoparticles: improving miltefosine stability and reducing its hemolytic potential toward erythrocytes and its cytotoxic effect on macrophages. *Biophys Chem* 2016; **217**: 20–31. <https://doi.org/10.1016/j.bpc.2016.07.005>
- 37** Valenzuela-Oses JK, García MC, Feitosa VA et al. Development and characterization of miltefosine-loaded polymeric micelles for cancer treatment. *Mater Sci Eng C* 2017; **81**: 327–33. <https://doi.org/10.1016/j.msec.2017.07.040>
- 38** Eissa MM, El-Moslemany RM, Ramadan AA et al. Miltefosine lipid nanocapsules for single dose oral treatment of *Schistosomiasis mansoni*: a preclinical study. *PLoS One* 2015; **10**: e0141788. <https://doi.org/10.1371/journal.pone.0141788>
- 39** Tan TRM, Hoi KM, Zhang P et al. Characterization of a polyethylene glycol-amphotericin B conjugate loaded with free AMB for improved antifungal efficacy. *PLoS One* 2016; **11**: e0152112.
- 40** Saldanha CA, Garcia MP, Iocca DC et al. Antifungal activity of amphotericin B conjugated to nanosized magnetite in the treatment of paracoccidioidomycosis. *PLoS Negl Trop Dis* 2016; **10**: e0004754. <https://doi.org/10.1371/journal.pntd.0004754>
- 41** Vu K, Weksler B, Romero I et al. Immortalized human brain endothelial cell line HCMEC/D3 as a model of the blood-brain barrier facilitates *in vitro* studies of central nervous system infection by *Cryptococcus neoformans*. *Eukaryot Cell* 2009; **8**: 1803–7. <https://doi.org/10.1128/EC.00240-09>
- 42** Nair KGS, Ramaiyan V, Sukumaran SK. Enhancement of drug permeability across blood brain barrier using nanoparticles in meningitis. *Inflammopharmacology* 2018; **26**: 675–84. <https://doi.org/10.1007/s10787-018-0468-y>
- 43** Kreuter J. Nanoparticulate systems for brain delivery of drugs. *Adv Drug Deliv Rev* 2012; **64**: 213–22. <https://doi.org/10.1016/j.addr.2012.09.015>
- 44** Ren T, Xu N, Cao C et al. Preparation and therapeutic efficacy of polysorbate-80-coated amphotericin B/PLA-b-PEG nanoparticles. *J Biomater Sci Polym Ed* 2009; **20**: 1369–80. <https://doi.org/10.1163/092050609X12457418779185>
- 45** Xu N, Gu J, Zhu Y et al. Efficacy of intravenous amphotericin B-polybutylcyanoacrylate nanoparticles against cryptococcal meningitis in mice. *Int J Nanomedicine* 2011; **6**: 905–13. <https://doi.org/10.2147/IJN.S17503>
- 46** Yukuyama MN, Ishida K, de Araujo GLB et al. Rational design of oral flubendazole-loaded nanoemulsion for brain delivery in cryptococcosis. *Colloids Surfaces A Physicochem Eng Asp* 2021; **630**: 127631. <https://doi.org/10.1016/j.colsurfa.2021.127631>
- 47** Chacko BJ, Palanisamy S, Gowrishankar NL et al. Effect of surfactant coating on brain targeting polymeric nanoparticles; a review. *Indian J Pharm Sci* 2018; **80**: 215–22. <https://doi.org/10.4172/pharmaceutical-sciences.1000348>

- 48** Spadari CC, Wirth F, Lopes LB *et al.* New approaches for cryptococcosis treatment. *Microorganisms* 2020; **8**: 613. <https://doi.org/10.3390/microorganisms8040613>
- 49** McClelland EE, Hobbs LM, Rivera J *et al.* The role of host gender in the pathogenesis of *Cryptococcus neoformans* infections. *PLoS One* 2013; **8**: e63632. <https://doi.org/10.1371/journal.pone.0063632>
- 50** Costa MC, Barros Fernandes H, Gonçalves GKN *et al.* 17- β -Estradiol increases macrophage activity through activation of the G-protein-coupled estrogen receptor and improves the response of female mice to *Cryptococcus gattii*. *Cell Microbiol* 2020; **22**: e13179. <https://doi.org/10.1111/cmi.13179>
- 51** Ahmad Z, Sharma S, Khuller GK. Chemotherapeutic evaluation of alginate nanoparticle-encapsulated azole antifungal and antitubercular drugs against murine tuberculosis. *Biol Med* 2007; **3**: 239–43. <https://doi.org/10.1016/j.nano.2007.05.001>
- 52** Martin-Villena MJ, Fernández-Campos F, Calpena-Campmany AC *et al.* Novel microparticulate systems for the vaginal delivery of nystatin: development and characterization. *Carbohydr Polym* 2013; **94**: 1–11. <https://doi.org/10.1016/j.carbpol.2013.01.005>